JBC Papers in Press. Published on May 9, 2012 as Manuscript M111.309492
The latest version is at http://www.jbc.org/cgi/doi/10.1074/jbc.M111.309492

# CHARACTERIZATION OF *CAULOBACTER CRESCENTUS* FTSZ

## USING DYNAMIC LIGHT SCATTERING

**Sen Hou,[1] Stefan A. Wieczorek,[1] Tomasz S. Kaminski,[1] Natalia Ziebacz,[1] Marcin Tabaka,[1] Nohemy A. Sorto,[2] Marie H. Foss,[3] Jared T. Shaw,[2] Martin Thanbichler,[4] Douglas B. Weibel,[3] Krzysztof Nieznanski,[5] Robert Holyst,[1*] Piotr Garstecki[1*]**

[1]Institute of Physical Chemistry PAS, Kasprzaka 44/52, 01-224 Warsaw, Poland

[2]Department of Chemistry, University of California at Davis, 1 Shields Ave, Davis, CA 95616 USA

[3]Department of Biochemistry, University of Wisconsin-Madison,
433 Babcock Drive, Madison, WI 53706, USA

[4]Max Planck Institute for Terrestrial Microbiology, LOEWE Center for Synthetic Microbiology and Faculty of Biology, Philipps University, D-35043 Marburg, Germany

[5]Department of Biochemistry, Nencki Institute of Experimental Biology,
Pasteur 3, 02-093 Warsaw, Poland

Address correspondence to: Piotr Garstecki, Robert Holyst, Institute of Physical Chemistry PAS, Kasprzaka 44/52, 01-224 Warsaw, Poland; E-mail: holyst@ptys.ichf.edu.pl (RH), garst@ichf.edu.pl (PG)

**Keywords:** bacteria; cytoskeleton; dynamic light scattering; electron microscopy (EM); protein self-assembly; C. crescentus; FtsZ; PC190723

**Background:** Self-assembly of the tubulin-homologue FtsZ is critical in bacterial cell division.

**Results:** Dynamic light scattering (DLS) measurements provide insight into the kinetics and stable length of *Caulobacter crescentus* FtsZ in vitro.

**Conclusion:** *Caulobacter crescentus* FtsZ forms short linear polymers in solution with the assembly rate depending on the concentrations of GTP and GDP.

**Significance:** DLS is a valuable technique for studying the polymerization of cytoskeletal proteins.

## SUMMARY

**The self-assembly of the tubulin homologue FtsZ at the mid-cell is a critical step in bacterial cell division. We introduce dynamic light scattering spectroscopy (DLS) as a new method to study the polymerization kinetics of FtsZ in solution. Analysis of the DLS data indicates that the FtsZ polymers are remarkably monodisperse in length, independent of the concentrations of GTP, GDP and FtsZ monomers. Measurements of the diffusion coefficient of the polymers demonstrate that their length is remarkably stable until the free GTP is consumed. We estimated the mean size of the FtsZ polymers within this interval of stable length to be between 9 and 18 monomers. The rate of FtsZ polymerization and depolymerization are likely influenced by the concentration of GDP, as the repeated addition of GTP to FtsZ increased the rate of polymerization and slowed down depolymerization. Increasing the FtsZ concentration did not change the size of FtsZ polymers; however, it increased the rate of the depolymerization reaction by depleting free GTP. Using transmission electron microscopy we observed that FtsZ forms linear polymers in solutions that rapidly convert to large bundles upon contact**



Copyright 2012 by The American Society for Biochemistry and Molecular Biology, Inc.

Downloaded from www.jbc.org by guest, on June 19, 2012

**with surfaces at time scales as short as several seconds. Finally, the best-studied small molecule that binds to FtsZ, PC190723, had no stabilizing effect on *C. crescentus* FtsZ filaments in vitro, which complements previous studies with *Escherichia coli* FtsZ and confirms that this class of small molecules binds Gram-negative FtsZ weakly.**

FtsZ is a widely conserved protein that is found in many species of Eubacteria, Archaea, and higher plants (1-6). FtsZ plays an important role in cell division in bacteria (7). During division, it forms polymers that assemble into a ring-like structure (the 'Z-ring') at the division plane (8-12). The Z-ring lines the inner face of the cytoplasmic membrane and guides the localization of other cell division proteins to establish the site of division and to initiate cytokinesis (13-14). The assembly of FtsZ polymers is triggered by binding to GTP (15). FtsZ polymerization is dynamic and terminates once free GTP is hydrolyzed to GDP (16).

As the earliest identified prokaryotic cytoskeletal protein (9), FtsZ has been widely studied by the bacterial cell biology community, and yet its polymer structure and in vivo mechanism of action are still not understood in detail. Real-time measurements of the kinetics of FtsZ polymerization and depolymerization may provide important mechanistic insight into the role of this protein in bacterial cell division.

FtsZ homologues from different organisms share significant structural similarity and yet have different biochemical and biophysical properties (17-19). For example, the small molecule PC190723 stabilizes FtsZ filaments from *Staphylococcus aureus* and *Bacillus subtilis* but not from *Escherichia coli* (17). It has been proposed that the reduced antibiotic activity of this compound against Gram-negative bacteria arises from its weak binding to FtsZ in Gram-negative organisms.

In this paper, we use dynamic light scattering (DLS) to study the polymerization kinetics of FtsZ from *C. crescentus*, a Gram-negative bacterium that due to its unique biphasic life cycle and asymmetric cell division has developed into a model organism for cell biological studies (18). The *C. crescentus* cell carries a single, polar flagellum during the swarmer phase. After differentiation into a stalked cell, division produces a cell containing a flagellum and a daughter cell with a stalk. We anticipate that studies of the polymerization of *C. crescentus* FtsZ will enhance our understanding of Z-ring formation and cell division in this bacterium.

DLS is a technique used to determine the distribution of the size of nucleotides and proteins (20) through the temporal correlation of the fluctuating intensity of scattered light (21). We anticipated that DLS could provide quantitative data on the kinetics of FtsZ polymerization and depolymerization *in vitro* that are not measurable with many other techniques that are often used to study protein assembly, including static light scattering (SLS) (22-24), transmission electron microscopy (TEM) (16) and atomic force microscopy (AFM) (25). SLS encompasses both single angle light scattering (SALS) and multiangle light scattering (MALLS). SALS measures the increase of the intensity of scattered light during polymerization, this signal does not convey information about the order of polymerization of FtsZ polymers (23). MALLS can be used to detect protein assembly by monitoring the molecular weight of the resulting filaments (24). It is best combined with off-line molecule fractionation techniques, such as capillary hydrodynamic chromatography (CHDF) and field flow fractionation (FFF) methods, to resolve not only the average molecular weight of the assemblies but also their distribution (26). TEM (16) and AFM (25) have been used to measure the length of FtsZ polymers adsorbed on surfaces. However, surface contact may enhance polymerization and bundle formation,

Downloaded from www.jbc.org by guest, on June 19, 2012

so that the observed FtsZ filaments may not represent the actual length of polymers suspended in bulk fluids or in the cell (27). Hence, it would be helpful to supplement AFM and TEM studies of FtsZ with techniques that provide dynamic information. In this paper we describe the first analysis of *C. crescentus* FtsZ structure and dynamics using DLS and demonstrate the capabilities of this biophysical technique for studying self-assembling proteins *in vitro*.

## RESULTS

*Characterization of the rate and degree of polymerization of FtsZ using DLS.* The decay time of the DLS signal is related to the coefficient of diffusion of objects that scatter light. In our study, an increase in the decay time provided a measure of polymerization, while depolymerization was inferred from the measured reduction of the decay time. This relationship is illustrated in Fig. 1a. Before addition of GTP, the decay time of FtsZ monomers was $\tau$ ~60 μs. Addition of GTP to a final concentration of 1 mM initiated polymerization, and within 10 min $\tau$ increased to ~200 μs. After 40 min the decay time started to decrease slowly, indicating the onset of FtsZ depolymerization.

There is no obvious correlation between the polymerization time (10 min) and the hydrolytic activity ($k_{cat}$ = 5.2 $min^{-1}$) of *C. crescentus* FtsZ (18). However, the value of $k_{cat}$ indicates the complete consumption of free GTP after ~ 47 min, which is in agreement with our results (for comparison see Fig. S4).

Apart from the decay time, DLS yields also the count rate that reflects the number of scattered photons detected by the detector per unit time. This readout provides information similar to that given by SLS (23). The count rate (Fig. 1b) acquired from a solution of FtsZ monomers was <10 kHz. The addition of GTP increased the count rate to 50 kHz within 10 min. After 40 min, the pool of free GTP was exhausted and the count rate fell again below 10 kHz. Thus, the count rate followed the same trend as the decay time throughout the polymerization process, which is consistent with previous SLS measurements of *E. coli* FtsZ (16,23).

We found that single-mode diffusion models could be accurately fit to the measured autocorrelation functions of our samples at all stages of the polymerization/depolymerization process (Fig. 1c-f), indicating that the polymers in the samples are monodisperse in length.

A comparison of our data with the results obtained for FtsZ homologues from other bacteria demonstrates significant differences in the rate of polymerization. For example, *E. coli* FtsZ was reported to polymerize completely within seconds (16); *Mycobacterium tuberculosis* FtsZ polymerizes completely within 1-10 min, depending on the pH (28-29). The polymerization time that we measured for *C. crescentus* FtsZ using DLS and SLS (Fig S1) was significantly longer.

Many factors may influence the rate of polymerization. For example, *Goley et al.* demonstrated that the polymerization of *C. crescentus* FtsZ is affected by buffer conditions (30). Interestingly, we observed that repeated cycles of polymerization and depolymerization as well as incubation with GDP before addition of GTP accelerated the rate of *C. crescentus* FtsZ polymerization (Fig S2).

*TEM analysis of FtsZ filaments.* In reported TEM procedures, samples containing polymerized FtsZ are typically brought in contact with carbon-coated copper grids for ~1 min before they are stained (18,23). In the first experiment, we deposited the sample (incubated with GTP for 1 min) on the grid surface, waited for 40 s, and then stained the resulting polymers with uranyl acetate. We found that the majority of the FtsZ polymers in this sample had formed flat bundles in which linear FtsZ filaments were

Downloaded from www.jbc.org by guest, on June 19, 2012

oriented in parallel to each other (Fig 2a). The bundles formed two-dimensional structures that lay flat on the grid surface. This arrangement suggests that polymerization and bundling largely occurred after FtsZ had contacted the surface, as bundles assembling in a bulk solution would produce more disordered, three-dimensional aggregates. To confirm this hypothesis, we incubated additional samples containing actively polymerizing FtsZ on the grid surface for only 1s before staining and dewetting with blotting paper. In this case, FtsZ only formed single protofilaments or small filament bundles consisting of only two parallel linear polymers (Fig 2b). We also prepared a sample that was fixed using 0.5% glutaraldehyde prior to its deposition on the grid and staining. In this sample, FtsZ primarily formed linear protofilaments that were shorter than those prepared using the other two protocols (Fig 2c).

The TEM data indicates that FtsZ assembles into bundles after contacting surfaces for as little as 1 s. The maximum length of the *C. crescentus* FtsZ polymers that we observed agrees with the length obtained for *E. coli* FtsZ filaments using AFM (27). However, the reported lengths of FtsZ polymers measured with TEM differ significantly; for example, a study of *E. coli* FtsZ polymers reported length > 1 μm (16). One explanation for this large discrepancy in the length of FtsZ filaments may be the contact of growing filaments with surfaces, which we found to have a profound effect on FtsZ polymer structure. FtsZ may adsorb on surfaces via weak electrostatic interactions (27). After adsorption, the two-dimensional diffusion of FtsZ along the surface may result in higher association rates compared to the three-dimensional diffusion in solution (31). The process should result in bundles of FtsZ filaments that are oriented with the plane of the surface and larger than in bulk solution, in agreement with our DLS and TEM measurements.

*Size of FtsZ polymers calculated by three fitting models.* An important advantage of DLS is that it allows the determination of the diffusion coefficient of FtsZ polymers (Fig 3a). Based on the diffusion coefficient and assuming that FtsZ polymers have an approximately linear shape (Fig 2), we used three different models to estimate their size (Fig. 3b) (32-34). The first model takes into consideration the anisotropy of diffusion of the rigid rod in three dimensions (32,35-36). To test the sensitivity of this model to specific assumptions about the diffusivity of the polymer, we applied a second algorithm, which uses an effective hydrodynamic radius of the rod (33). Finally, we used a third model in which the FtsZ polymer consists of identical spheres and has an overall rough surface (34). All of the models yield the number of monomers in the polymer, and all three of them produce similar results: the polymers ranged from 9 to 18 monomers in length in the stable interval (Fig. 3b).

Using the DLS readout of the diffusion coefficient we calculated the size of the monomer of *C. crescentus* FtsZ to be 5.17±0.56 nm. This agrees well with the reported size of 5-6 nm of the *E. coli* FtsZ (37). The length of a the polymer containing 9 to 18 monomers thus ranges between ~ 47 and 93 nm and is in close agreement with our TEM data (Fig 2c).

Notably, our data suggests that the number of monomers in the *C. crescentus* FtsZ polymer is much smaller than in the *E. coli* FtsZ (roughly 70 monomers) (38). Since the sizes of the monomers of *C. crescentus* FtsZ and *E. coli* FtsZ are almost equal, the calculated length of *C. crescentus* FtsZ polymer is much shorter than that of *E. coli* FtsZ polymer. This result well agrees with reported TEM images, which show that *C. crescentus* FtsZ polymers are much shorter than *E. coli* FtsZ polymers (18,37).

As an additional check we verified that the assumption of the morphology of straight rigid rods does not significantly influence the above estimations. Indeed the TEM scans (Fig 2)

Downloaded from www.jbc.org by guest, on June 19, 2012

show that the FtsZ filaments may be slightly curved. In order to gauge the influence of the shape on the estimated length of the filaments, we used two additional models based on the extreme assumptions of a C- or S-shaped chains. These models provided similar estimates of the length of the FtsZ polymers—to within one monomer (see supporting information)—and confirm the above estimates.

From the variation of the diffusion coefficient of FtsZ polymers, we deduced that *C. crescentus* FtsZ assembles very rapidly into a filament consisting of ~5 monomers. The subsequent elongation of this filament occurs significantly more slowly. The diffusion coefficient initially dropped to ~40% of that of a monomer within 1 min after the start of polymerization. In the following 9 min, it then gradually decreased to its minimum value, reaching ~30% of the value measured for the monomer.

*Influence of the GTP/GDP ratio on FtsZ polymerization and depolymerization.* We used the same experimental system to measure changes of the kinetics of polymerization and depolymerization of FtsZ polymers upon successive additions of GTP. We added GTP into the FtsZ polymerization buffer solution to a final concentration of 0.25 mM. In the course of the experiment, GTP was completely converted to GDP, resulting in disassembly of the polymers. We then titrated-in GTP again (to its initial concentration) and iterated this procedure three times (Fig. 4). The decay time, the count rate and the diffusion coefficient displayed similar curves after each addition of GTP. Notably, the diffusion coefficient of the protofilaments did not change between the successive experiments. However, after consecutive additions of nucleotide, FtsZ polymerization was accelerated, while depolymerization was decelerated. For example, after the first addition of GTP polymerization occurred within ~20 min and complete polymer disassembly within ~10 min. After the fourth addition of GTP, FtsZ polymerization was instantaneous (within the resolution of our measurements), whereas the depolymerization phase was extended to ~20 min. We associate the observed increase of the rate of polymerization with the gradual accumulation of GDP. Consistent with this idea, an assay in which we directly mixed GTP and GDP to emulate the conditions just before the fourth addition of GTP in the experiment described above showed the same result (see Fig S2).

Our results are consistent with a previous study showing that the disassembly rate of *E. coli* FtsZ decreases with increasing GDP concentrations (23). Similarly, the stimulatory effect of GDP on the assembly reaction observed for *C. crescentus* FtsZ may also apply to homologues from other species, including *E. coli* (23). However, this phenomenon may so far have escaped detection for *E. coli* FtsZ due to its very rapid rate of polymerization (23).

*Influence of GTP concentration on FtsZ polymerization.* Our polymerization experiments produced FtsZ filaments of the same length irrespective of the GTP concentration. We also found that the GTP concentration did not affect the rate of FtsZ polymerization/ depolymerization (Fig. 5). As we show in the supporting information, the viscosity of FtsZ solutions did not change appreciably during the polymerization step. Higher concentrations of GTP only prolonged the interval during which the FtsZ polymers remained at their maximum length. These results agree with a previous study of the influence of GTP on the polymerization of *E. coli* FtsZ (16).

*Influence of FtsZ concentration on FtsZ polymerization.* We demonstrate that the concentration of FtsZ clearly influences the interval during which the polymers are stable, presumably because it affects the time required for the complete consumption of GTP. However, within the limited range of FtsZ concentrations tested (0.22-0.44 mg/mL), it did not change the

Downloaded from www.jbc.org by guest, on June 19, 2012

maximum length of the filaments, as derived from the invariance of the diffusion coefficients measured (Fig 6). High concentrations of FtsZ thus merely increased the number of FtsZ polymers, but did not increase their length. Importantly, the critical concentration of *C. crescentus* FtsZ, i.e. the minimum concentration required for proper assembly, was measured to be 0.52 μM (see supporting information). The concentration of FtsZ tested in our experiments was always well above this value.

*Influence of PC190723 on the polymerization of C. crescentus FtsZ.* PC190723 is a phenylthiazoline that prevents cell division by stabilizing FtsZ filaments and reducing the GTPase activity of this protein (17). PC190723 is an effective antibiotic against both methicillin-resistant and multi-drug resistant *S. aureus* strains; however it has much weaker activity against Gram-negative bacteria (17). One hypothesis has been that this compound binds only weakly to Gram-negative FtsZ, which is supported by experiments with *E. coli* FtsZ in vitro (17). The verification of this hypothesis would benefit greatly from studies with FtsZ from another Gram-negative bacterium. With synthetic PC190723 in-hand (39), we studied the interaction of this small molecule with *C. crescentus* FtsZ in vitro using DLS.

Our measurements indicate that PC190723 has no effect on the polymerization of *C. crescentus* FtsZ (Fig. 7). The decay time increased and the count rate decreased to the same extent in the presence and absence of PC190723, respectively. Similarly, all characteristics of the polymerization and depolymerization kinetics – including the polymerization rate, the interval during which the polymers retained their maximum length, the size of polymers as indicated by their diffusion coefficient, and the depolymerization rate – remained unaffected by PC190723.

## CONCLUSIONS

We used dynamic light scattering to study the polymerization and disassembly of FtsZ polymers. This technique enabled us to measure the increase of the intensity of scattered light and the characteristic decay time of the autocorrelation function, and provided a quantitative value for the degree of FtsZ polymerization.

We envision that the methodological framework established in this study has laid the foundation for the application of this technique to various other cytoskeletal proteins.

## MATERIALS AND METHODS

*Reagents. C. crescentus* FtsZ was overproduced and purified as described previously (18). We determined the concentration of FtsZ via a BCA assay using an Ocean Optics USB 2000+ spectrometer and a BCA assay kit from Sigma-Aldrich, Poland. GTP and GDP were from Sigma-Aldrich, Poland. PC190723 ($C_{14}H_8ClF_2N_3O_2S$, MW=355.75) was synthesized according to a previously published protocol (39). PC190723 was diluted in DMSO to a concentration of 1 mM before use.

*Polymerization of FtsZ.* Since *C. crescentus* cells are routinely cultured at 28-30 °C, we kept the temperature of FtsZ polymerization assays at 29 °C. The polymerization buffer consisted of 50 mM MES-NaOH, 10 mM $MgCl_2$, and 50 mM KCl (pH 6.5). The concentration of FtsZ in our experiments was 220 mg/L (4.1 μM; MW = 54.2 kDa). A concentrated solution of GTP (0.1 M) was added to the FtsZ solution to initiate polymerization, thus minimizing the change in volume (1 mL). We also performed control experiments in a buffer containing only 3 mM $MgCl_2$, which yielded very similar results (Fig. S3).

*DLS measurements.* We used a Brookhaven BI-200SM Goniometer equipped with Contin software to measure DLS spectra. A stable Argon ion laser with a wavelength of 514 nm was used for DLS measurements.

All samples were filtered through a 0.22 μm



Downloaded from www.jbc.org by guest, on June 19, 2012

filter before analysis. In each experiment, we mixed the GTP solution with the FtsZ solution and placed the reaction mixture in the goniometer for DLS measurements. We began to calculate the reaction time once the GTP was added into the FtsZ solution.

We measured the intensity of scattered light at an angle of 90° and used the Contin software to analyze the data for the distribution of size of the FtsZ polymers. We found that we needed to accumulate the signal for 1 min to minimize the measurement error.

*Transmission electron microscopy.* A solution of GTP was added to the FtsZ solution to a final concentration of 1 mM to initiate polymerization. After 15 min of incubation at 29 °C in the presence of GTP, 20-µl samples were placed on 400-mesh copper grids (Sigma, St. Louis, MO, USA) covered with collodion (SPI Supplies, West Chester, PA, USA) and carbon (in additional experiments, the samples were fixed prior to deposition on the grid by incubation with 0.5% glutaraldehyde for 10 min). The samples deposited on the grid were either incubated for 40 s or immediately adsorbed on the surface by dewetting with blotting paper (corresponding to a contact time of ~1 s). Subsequently, negative staining was performed with 2% (w/v) uranyl acetate (SPI Supplies) for 25 s. The grids were examined at an acceleration voltage of 80 kV in a JEM 1400 electron microscope (JEOL Co., Japan) equipped with a digital camera (CCD MORADA, SiS-Olympus, Germany)

*Calculation of the decay time.* The system records the intensity *I(q,t)* of light scattered along vector *q* as a function of time. The size of the FtsZ polymers was extracted from the autocorrelation of *I(t)*. The normalized autocorrelation function is:

$$g(q,t) = \frac{< I(q,0)I(q,t) >}{< I(q,0) >^2} - 1 \qquad (1)$$

The scattering vector was determined by the refractive index of the solution (*m*), the wavelength ($\lambda$) of the incident light, and the scattering angle $\theta = 90°$:

$$q = \frac{4\pi m}{\lambda} \sin\frac{\theta}{2} \qquad (2)$$

We used a standard Abbe refractometer (Carl-Zeiss, Germany) to measure the refractive index, *m*, of the FtsZ solution. We found that *m* = 1.335, which was approximately constant during the polymerization of FtsZ. Thus, *q* was also constant when the scattering angle $\theta$ was fixed.

If the scattered field obeys Gaussian statistics, the measured intensity autocorrelation function *g*(q,t) is related to the normalized field correlation function $g'$ (q,t)

$$g(q,t) = c\left|g'(q,t)\right|^2 \qquad (3)$$

where $c \in (0, 1)$ is the experimental coherence factor. If the fluctuation of the concentration of the polymer relaxes through simple Brownian diffusion, *g′*(q,t) can be expressed by a one-component diffusion mode:

$$g'(q,t) = \exp(-\frac{t}{\tau}) \qquad (4)$$

where $\tau$, which we refer to as the 'decay time', is the characteristic time of the decay of autocorrelation of the signal. Combining Eq. 3 and 4 connects the decay time to the autocorrelation function:

$$g(q,t) = c\exp(-t/\tau)^2 \qquad (5)$$

Fitting Eq. 5 to the experimental data made it possible to determine the decay time of FtsZ polymers.

Further, we use the decay time $\tau$ to extract the diffusion coefficient *Dp* of the FtsZ polymers

$$D_p = \frac{1/\tau}{q^2} \qquad (6)$$

*Determination of the size of FtsZ polymers.* Three traditional fitting methods (32-34) were



Downloaded from www.jbc.org by guest, on June 19, 2012

used to calculate the size of FtsZ polymers.

In the first method, the translational self-diffusion coefficient $D_p$ of a cylindrical polymer can be expressed as (33)

$$D_p = \frac{1}{3}(D_{II} + 2D_{\perp}) \qquad (7)$$

where $D_{\perp}$ and $D_{II}$ describe the diffusion perpendicular and parallel to the long axis of the cylinder, respectively.

$$D_{\perp} = \frac{k_B T}{4\pi\eta L}(\ln(\rho) + v_{\perp}) \qquad (8)$$

$$D_{II} = \frac{k_B T}{2\pi\eta L}(\ln(\rho) + v_{II}) \qquad (9)$$

In Eq. 8 and 9, $k_B$ is the Boltzmann constant, $T$ is the absolute temperature, $\eta$ is the viscosity of the FtsZ solution, $\rho$ is axial ratio, and $v_{\perp}$ and $v_{II}$ are "end-effect corrections".

$$v_{\perp} = 0.839 + 0.185/\rho + 0.233/\rho^2 \qquad (10)$$

$$v_{II} = -0.207 + 0.980/\rho - 0.133/\rho^2 \qquad (11)$$

$$\rho = \frac{L}{d} = n \qquad (12)$$

where n is the number of monomers in a polymer, $L$ and $d$ are the length and diameter of the FtsZ polymer, respectively. We assume that FtsZ polymers consist of a single filament of monomers. Combining Eqs. 7-11 we obtain an expression for the coefficient of diffusion of a single polymer:

$$D_p = \frac{k_B T}{6\pi\eta L}(2\ln(n) + v_{\perp} + v_{II}) \qquad (13)$$

If n>5, $v_{\perp}$+ $v_{II}$ can be closely approximated by 0.632 according to Eq. 10 and 11, yielding:

$$D_p = \frac{k_B T}{3\pi\eta L}(\ln(n) + 0.316) \qquad (14)$$

Eq. 12 can be written as:

$$L = dn \qquad (15)$$

Inserting Eq. 15 into Eq. 14, we obtain an expression relating $D_p$ with the number of monomers in the oligomer:

$$D_p = \frac{k_B T}{3\pi\eta d} \cdot \frac{\ln(n) + 0.316}{n} \qquad (16)$$

Eq. 16 is only valid for FtsZ filaments consisting of n >5 monomers. The diffusion coefficient $D_m$ of a monomer according to the Stokes-Sutherland-Einstein equation is:

$$D_m = \frac{k_B T}{3\pi\eta d} \qquad (17)$$

Here the viscosity of FtsZ solutions $\eta$ does not change during the polymerization process (see supporting information on viscosity data, Fig S5). Moreover, $q$ in Eq. 6 is also a constant due to a constant refractive index $m$ and a fixed scattering angle $\theta$. Combining Eq. 6, 16, and 17, we can express the ratio of the decay times of the polymer $\tau_{0p}$ (for n >5) and of the monomer $\tau_{0m}$ solely as a function of the number of monomers in a polymer:

$$\frac{\tau_{0m}}{\tau_{0p}} = \frac{\ln(n) + 0.316}{n} \qquad (18)$$

Eq. 18 enables us to extract the length of the polymers $n$ directly from the analysis of the autocorrelation functions of the DLS signal.

In the second method (32), the effective hydrodynamic radius of a thread polymer $R_{hp}$ is expressed as

$$R_{hp} = \frac{L}{2s - 0.19 - 8.24/s + 12/s^2} \qquad (19)$$

where $s$ is defined as

$$s = \ln(L/r) = \ln(2n) \qquad (20)$$

where $r$ is the radius of thread filament (here is the radius of monomers) and $n$ is the number of monomers in a polymer.

Based on the Stokes-Sutherland-Einstein equation, the diffusion coefficient of the polymer $D_p$ can be expressed as



Downloaded from www.jbc.org by guest, on June 19, 2012

$$D_p = \frac{k_B T}{6\pi\eta R_{hp}} \quad (21)$$

and the diffusion coefficient of the monomer $D_m$ is expressed as

$$D_m = \frac{k_B T}{6\pi\eta r} \quad (22)$$

Combining Eqs. 6, 21 and 22 we determine that

$$\frac{\tau_{0m}}{\tau_{0p}} = \frac{r}{R_{hp}} \quad (23)$$

Substituting Eqs. 19 and 20 into Eq. 23, we derive

$$\frac{\tau_{0m}}{\tau_{0p}} = \frac{2\ln(2n) - 0.19 - 0.84/\ln(2n) + 12/\ln^2(2n)}{2n} \quad (24)$$

Eq. 24 enables us to extract the length of the polymers $n$ directly from the analysis of the autocorrelation functions of the DLS signal.

In the third method the FtsZ polymer is assumed to comprise identical spheres. According to Kirkwood formulation (34), the diffusion coefficient of such a polymer is

$$D_p = k_B T / f \quad (25)$$

where $f$ is the frictional coefficient tensor defined as

$$f = \left(6\pi\eta \sum_{l=1}^{n} r_l\right)[1 + (1/\sum_{l=1}^{n} r_l)\sum_{l=1}^{n}\sum_{s=1}^{n} r_l r_s < R_{ls}^{-1} >]^{-1} \quad (26)$$

where $r$ is the radius of subunit $l$ and $R_{ls}$ is the distance between the $l$-th and $s$-th unit ($l \neq s$). For a polymer composed of identical spherical subunits, Eq 26 reduces to:

$$f = (6\pi\eta n r)[1 + \frac{1}{2n}\sum_{l=1}^{n}\sum_{s=1}^{n}\frac{1}{|l-s|}]^{-1} \quad (27)$$

The sum can be approximated by:

$$\begin{aligned} &\tfrac{1}{2}\textstyle\sum_{l=1}^{n}\sum_{s=1}^{n}\frac{1}{|l-s|} = \sum_{s=1}^{n-1}(\frac{n-s}{s}) \\ &= n(\textstyle\sum_{s=1}^{n}\frac{1}{s} - 1) \\ &\approx n\left(ln(n) + \gamma - 1 + \frac{1}{2n} - \sum_{k=1}^{\infty}\frac{B_{2k}}{2kn^{2k}}\right) \\ &\approx n(ln(n) + \gamma - 1), \text{ for } \; n > 5 \end{aligned} \quad (28)$$

where $B_k$ are the Bernoulli numbers and $\gamma$=0.5772 is the Euler–Mascheroni constant. Combining Eqs 27 and 28 one obtains:

$$\begin{aligned} f &= 6\pi\eta r \frac{n}{0.5772 + ln(n)} \\ &= 3\pi\eta d \frac{n}{0.5772 + ln(n)} \end{aligned} \quad (29)$$

Further, combining Eqs 25 and 29 we obtain:

$$D_p = \frac{k_B T}{3\pi\eta d}\frac{0.5772 + ln(n)}{n} \quad (30)$$

and combining Eqs 6, 17 and 30, we get

$$\frac{\tau_{0m}}{\tau_{0p}} = \frac{\ln(n) + 0.5772}{n} \quad (31)$$

Eq. 31 enables us to extract the number $n$ of monomers in the polymer directly from the analysis of the autocorrelation functions of the DLS signal.

## REFERENCES


1. Kiessling, J., Kruse, S., Rensing, S. A., Harter, K., Decker, E. L., and Reski, R. (2000) *J. Cell Biol.* **151**, 945-950
2. Paez, A., Tarazona, P., Mateos-Gil, P., and Velez, M. (2009) *Soft Matter* **5**, 2625-2637
3. Li, Z., Trimble, M. J., Brun, Y. V., and Jensen, G. J. (2007) *EMBO J.* **26**, 4694-4708
4. Margalit, D. N., Romberg, L., Mets, R. B., Hebert, A. M., Mitchison, T. J., Kirschner, M. W., and RayChaudhuri, D. (2004) *Proc. Natl. Acad. Sci. U. S. A.* **101**, 13969-13969
5. Erickson, H. P., Anderson, D. E., and Osawa, M. (2010) *Microbiol. Mol. Biol. Rev.* **74**, 504-528
6. Erickson, H. P., and Chen, Y. D. (2011) *Biochemistry (Mosc.)* **50**, 4675-4684
7. Romberg, L., and Levin, P. A. (2003) *Annu. Rev. Microbiol.* **57**, 125-154




Downloaded from www.jbc.org by guest, on June 19, 2012

8. Addinall, S. G., and Lutkenhaus, J. (1996) *Mol. Microbiol.* **22**, 231-237
9. Bi, E., and Lutkenhaus, J. (1991) *Nature* **354**, 161-164
10. Harry, E. J. (2001) *Mol. Microbiol.* **40**, 795-803
11. Levin, P. A., and Weart, R. B. (2003) *J. Bacteriol.* **185**, 2826-2834
12. Brun, Y. V., and Quardokus, E. M. (2002) *Mol. Microbiol.* **45**, 605-616
13. Goehring, N. W., and Beckwith, J. (2005) *Curr. Biol.* **15**, R514-R526
14. Jensen, G. J., Li, Z., Trimble, M. J., and Brun, Y. V. (2007) *EMBO J.* **26**, 4694-4708
15. Nogales, E., Downing, K. H., Amos, L. A., and Lowe, J. (1998) *Nat. Struct. Biol.* **5**, 451-458
16. Mukherjee, A., and Lutkenhaus, J. (1999) *J. Bacteriol.* **181**, 823-832
17. Andreu, J. M., Schaffner-Barbero, C., Huecas, S., Alonso, D., Lopez-Rodriguez, M. L., Ruiz-Avila, L. B., Nunez-Ramirez, R., Llorca, O., and Martin-Galiano, A. J. (2010) *J. Biol. Chem.* **285**, 14239-14246
18. Thanbichler, M., and Shapiro, L. (2006) *Cell* **126**, 147-162
19. Panda, D., Beuria, T. K., Krishnakumar, S. S., Sahar, S., Singh, N., Gupta, K., and Meshram, M. (2003) *J. Biol. Chem.* **278**, 3735-3741
20. Hou, S., Ziebacz, N., Wieczorek, S. A., Kalwarczyk, E., Sashuk, V., Kalwarczyk, T., Kaminski, T. S., and Holyst, R. (2011) *Soft Matter* **7**, 6967-6972
21. Koppel, D. E. (1972) *J. Chem. Phys.* **57**, 4814-4820
22. Popp, D., Iwasa, M., Erickson, H. P., Narita, A., Maeda, Y., and Robinson, R. C. (2010) *J. Biol. Chem.* **285**, 11281-11289
23. Small, E., and Addinall, S. G. (2003) *Microbiology* **149**, 2235-2242
24. Casini, G. L., Graham, D., Heine, D., Garcea, R. L., and Wu, D. T. (2004) *Virology* **325**, 320-327
25. Mingorance, J., Tadros, M., Vicente, M., Gonzalez, J. M., Rivas, G., and Velez, M. (2005) *J. Biol. Chem.* **280**, 20909-20914
26. Wyatt, P. J. (1998) *J. Colloid Interface Sci.* **197**, 9-20
27. Hamon, L., Panda, D., Savarin, P., Joshi, V., Bernhard, J., Mucher, E., Mechulam, A., Curmi, P. A., and Pastre, D. (2009) *Langmuir* **25**, 3331-3335
28. White, E. L., Ross, L. J., Reynolds, R. C., Seitz, L. E., Moore, G. D., and Borhani, D. W. (2000) *J. Bacteriol.* **182**, 4028-4034
29. Chen, Y. D., Andersen, D. E., Rajagopalan, M., and Erickson, H. P. (2007) *J. Biol. Chem.* **282**, 27736-27743
30. Goley, E. D., Dye, N. A., Werner, J. N., Gitai, Z., and Shapiro, L. (2010) *Mol. Cell* **39**, 975-987
31. Berg, O. G., and von Hippel, P. H. (1985) *Annu. Rev. Biophys. Biophys. Chem.* **14**, 131-160
32. Van de Sande, W., and Persoons, A. (1985) *J. Phys. Chem.* **89**, 404-406
33. Seils, J., and Pecora, R. (1995) *Macromolecules* **28**, 661-673
34. Bloomfield.V, Dalton, W. O., and Van Holde, K. E. (1967) *Biopolymers* **5**, 135-148
35. Tirado, M. M., and Garcia de la Torre, J. (1980) *J. Chem. Phys.* **73**, 1986-1993
36. Tirado, M. M., and Garcia de la Torre, J. (1979) *J. Chem. Phys.* **71**, 2581-2587
37. Gonzalez, J. M., Velez, M., Jimenez, M., Alfonso, C., Schuck, P., Mingorance, J., Vicente, M., Minton, A. P., and Rivas, G. (2005) *Proc. Natl. Acad. Sci. U. S. A.* **102**, 1895-1900
38. Reija, B., Monterroso, B., Jimenez, M., Vicente, M., Rivas, G., and Zorrilla, S. (2011) *Anal. Biochem.* **418**, 89-96
39. Sorto, N. A., Olmstead, M. M., and Shaw, J. T. (2010) *J. Org. Chem.* **75**, 7946-7949

## FOOTNOTES



Downloaded from www.jbc.org by guest, on June 19, 2012

*The work was supported by Collaborative Research Grant from the Human Frontier Science Program (RGY0069/2008-C103 to P.G., M.T., and D.B.W.) and within the programs co-financed by the EU "European Regional Development Fund": NanoFun POIG.02.02.00-00-025/09 and TEAM/2008-2/2 (operated by the Foundation for Polish Science). The National Institutes of Health (USA) is acknowledged for funding to JTS (R01AI08093). Microscopic studies were performed in the Laboratory of Electron Microscopy (Nencki Institute of Experimental Biology, Warsaw, Poland) using equipment installed within the project sponsored by the EU Structural Funds: Centre of Advanced Technology BIM - Equipment purchase for the Laboratory of Biological and Medical Imaging.

Key words: FtsZ, transmission electron microscopy, *C. crescentus*, dynamic light scattering, PC190723, viscosity

Downloaded from www.jbc.org by guest, on June 19, 2012

## FIGURE LEGENDS

**Fig. 1.** Decay time (a) and count rate (b) of FtsZ polymers as a function of FtsZ polymerization time. GTP was added to a final concentration of 1 mM to initiate polymerization. The concentration of FtsZ was 220 mg/L. (c-f) The panels show the one-component fitting of DLS data (see methods section for explanation) to Eq. 5 of the points labeled c-f in Fig. 1 a. The data demonstrates the uniformity in the length of FtsZ polymers during polymerization.

**Fig. 2.** (a) TEM image of FtsZ polymers incubated on the grid surface for 40s, prior to be stained by uranyl acetate. (b) TEM image of FtsZ polymers incubated on the grid surface for 1s, prior to be stained by uranyl acetate. (c) TEM image of FtsZ polymers fixed with 0.5% glutaraldehyde for 10 min and then incubated on the grids surface for 40s, followed by being stained with uranyl acetate. (d), (e) and (f) are cartoons depicting FtsZ bundles, linear FtsZ polymers, and small FtsZ bundles, indicating that a short-time contacting with a surface greatly enhances the formation of FtsZ bundles. All samples were incubated at 29 °C for 15 min before contacting with the grid surface. Scale bar is 200 nm.

**Fig. 3.** Diffusion coefficient (a) and size (b) of FtsZ polymers (expressed as the number of FtsZ monomers in a polymer) as a function of FtsZ polymerization time. GTP was added to a final concentration of 1 mM to initiate polymerization. The concentration of FtsZ was 220 mg/L. We show the size of FtsZ polymers by the result of three fitting methods. The diameter of one monomer is 5.17±0.56 nm.

**Fig. 4.** Decay time (a), count rate (b) and diffusion coefficient (c) of FtsZ polymers as a function of FtsZ polymerization time over four assembly/disassembly cycles. Each cycle is started by addition of 0.25 mM GTP (final concentration) to the FtsZ solution. The concentration of FtsZ was 220 mg/L.

**Fig. 5.** Influence of GTP concentration on the decay time (a) and diffusion coefficient (b) of FtsZ polymers during FtsZ polymerization process. A high GTP concentration prolonged the time over which FtsZ polymers are stable. The concentration of FtsZ was 220 mg/L.

**Fig. 6.**(a) Influence of the concentration of FtsZ monomers on the diffusion coefficient of resulting FtsZ polymers during the polymerization process. The size of FtsZ polymers (expressed as the number of FtsZ monomers in a polymer) was calculated using three methods: model 1 (b), model 2 (c) and model 3 (d). GTP was added to a final concentration of 1 mM to initiate polymerization. The diameter of one monomer is 5.17±0.56 nm.

**Fig. 7.** Count rate (a), decay time (b) and diffusion coefficient (c) of FtsZ polymers as a function of polymerization time. The data demonstrate that PC190723 does not influence FtsZ polymerization. GTP was added to a final concentration of 1 mM to initiate the polymerization. The concentration of FtsZ was 220 mg/L. The concentration of PC190723 was 20 μM (7.1 μg/mL). The same volume of DMSO as of the PC190723 solution was used as a control.

Downloaded from www.jbc.org by guest, on June 19, 2012

**Figure 1**

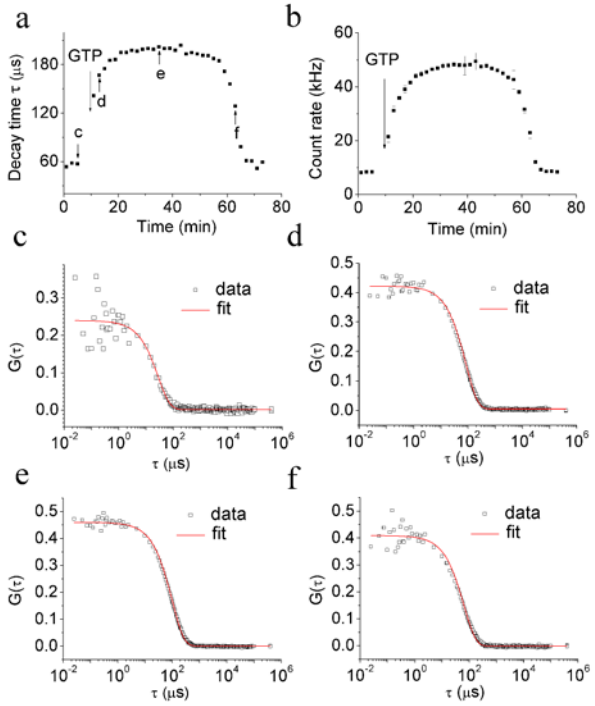


**Figure 2**

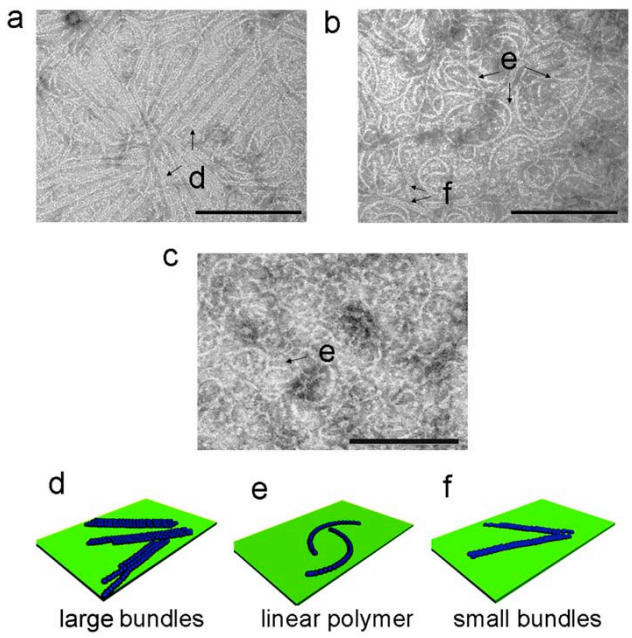


Downloaded from www.jbc.org by guest, on June 19, 2012

**Figure 3**

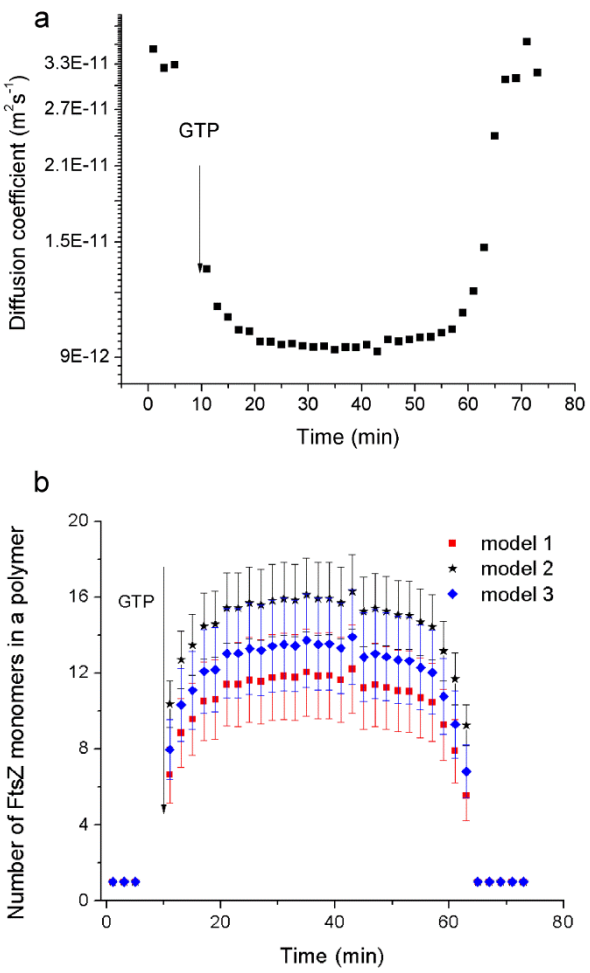


**Figure 4**

Downloaded from www.jbc.org by guest, on June 19, 2012

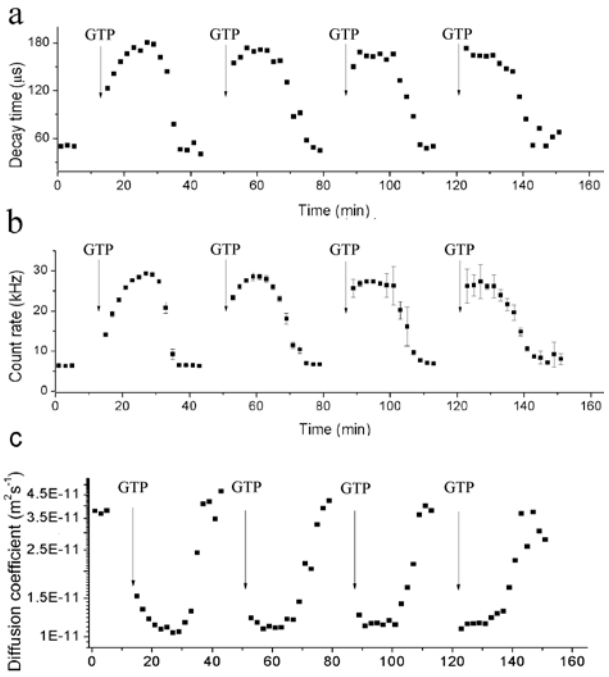


**Figure 5**

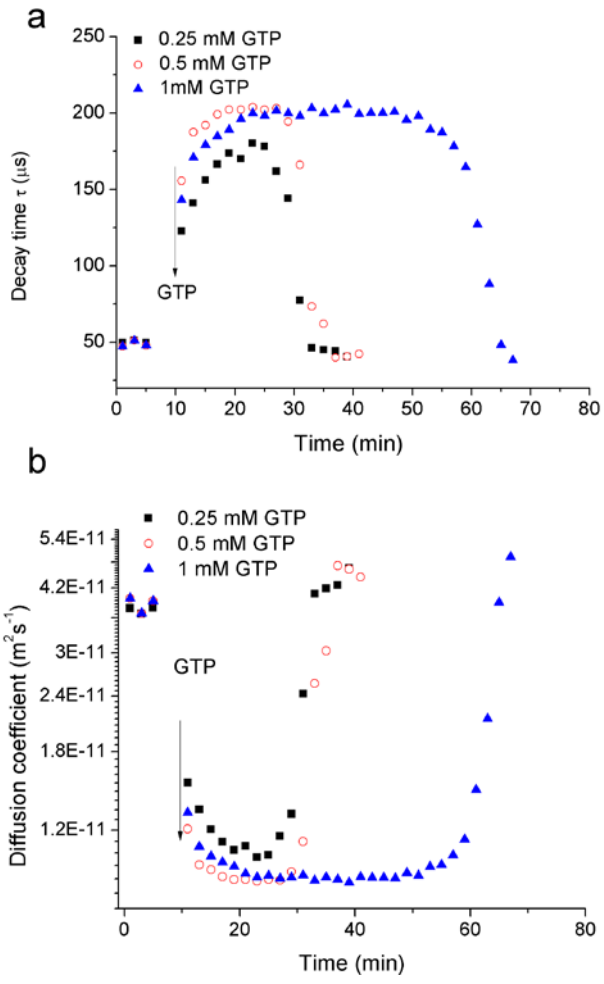


Downloaded from www.jbc.org by guest, on June 19, 2012

**Figure 6**

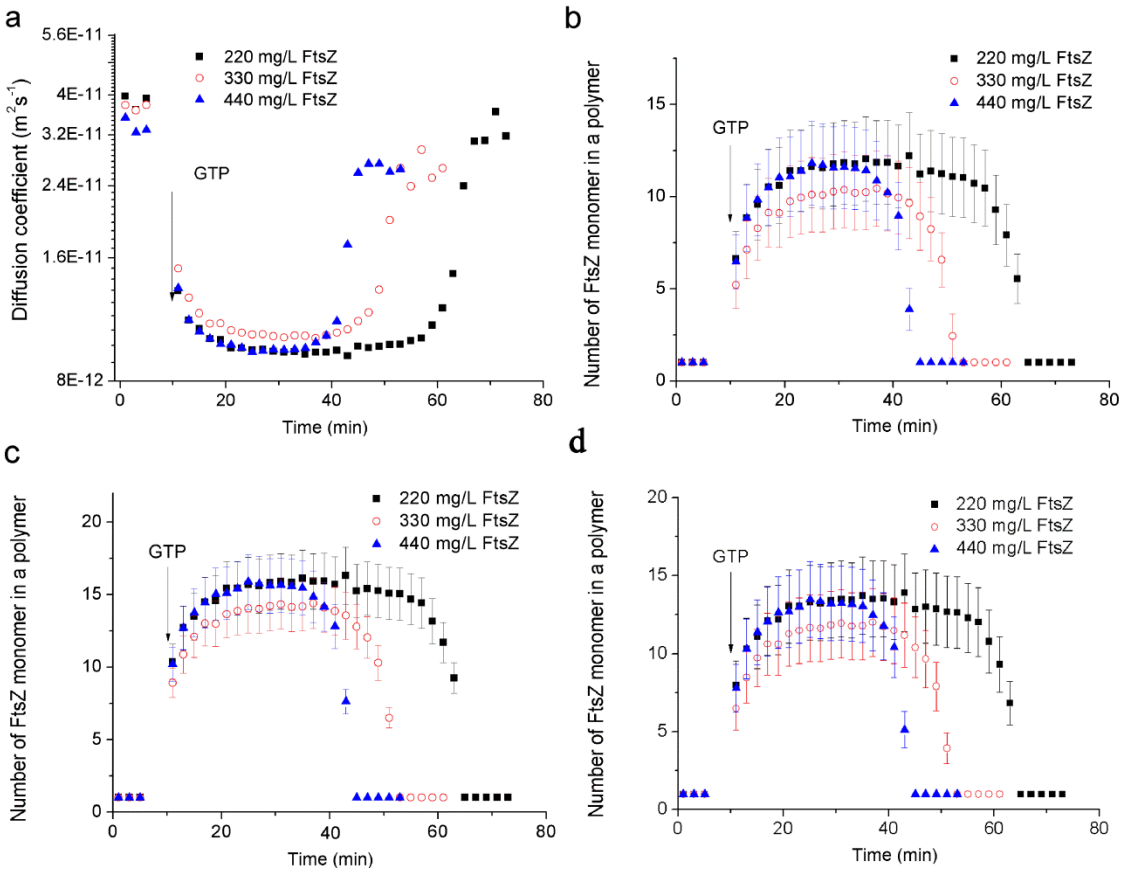


Downloaded from www.jbc.org by guest, on June 19, 2012

**Figure 7**

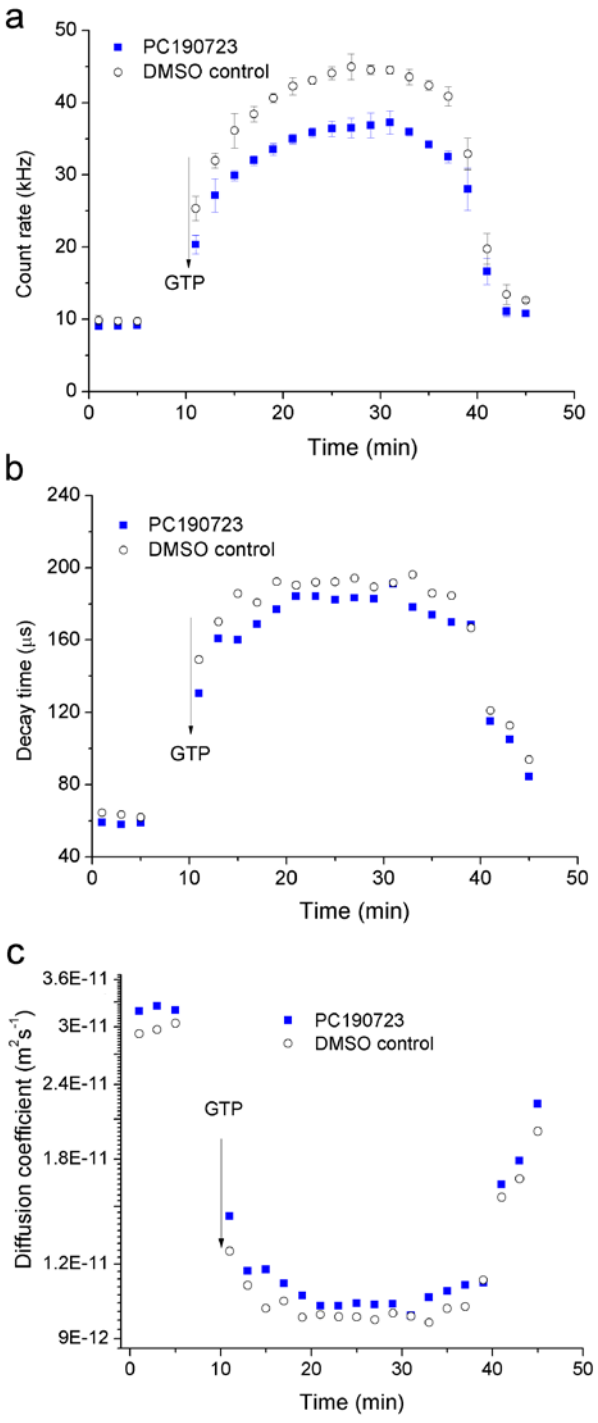


Downloaded from www.jbc.org by guest, on June 19, 2012